Developmental Biology 460 (2020) 2–11

Contents lists available at ScienceDirect

Developmental Biology

journal homepage: www.elsevier.com/locate/developmentalbiology

Pattern formation mechanisms of self-organizing reaction-diffusion systems

Amit N. Landge [a], Benjamin M. Jordan [b], Xavier Diego [c], Patrick Müller [a,d,*]

[a] Systems Biology of Development Group, Friedrich Miescher Laboratory of the Max Planck Society, 72076, Tübingen, Germany
[b] Department of Organismic and Evolutionary Biology, Harvard University, Cambridge, MA, 02143, USA
[c] European Molecular Biology Laboratory, Barcelona Outstation, 08003 Barcelona, Spain
[d] Modeling Tumorigenesis Group, Translational Oncology Division, Eberhard Karls University Tübingen, 72076, Tübingen, Germany

A B S T R A C T

Embryonic development is a largely self-organizing process, in which the adult body plan arises from a ball of cells with initially nearly equal potency. The reaction-diffusion theory first proposed by Alan Turing states that the initial symmetry in embryos can be broken by the interplay between two diffusible molecules, whose interactions lead to the formation of patterns. The reaction-diffusion theory provides a valuable framework for self-organized pattern formation, but it has been difficult to relate simple two-component models to real biological systems with multiple interacting molecular species. Recent studies have addressed this shortcoming and extended the reaction-diffusion theory to realistic multi-component networks. These efforts have challenged the generality of previous central tenets derived from the analysis of simplified systems and guide the way to a new understanding of self-organizing processes. Here, we discuss the challenges in modeling multi-component reaction-diffusion systems and how these have recently been addressed. We present a synthesis of new pattern formation mechanisms derived from these analyses, and we highlight the significance of reaction-diffusion principles for developmental and synthetic pattern formation.

1. Introduction

Patterns are ubiquitous in nature – from the molecular arrangements in crystals and snowflakes to the dynamics of societies and the formation of galaxies. Many of these spatial patterns are strikingly similar across orders of magnitude in length scales, but it is currently largely unclear whether equivalent patterns are formed by similar self-organizing mechanisms. Numerous theories have been put forward with the goal to unravel the principles of pattern formation (reviewed in Roth, 2011), but few of them are as universal as the theory of reaction-diffusion (RD) systems first proposed by Alan Turing (1952). Turing's theory explains the complex self-organizing mechanisms underlying embryonic patterning using simple reactions of just two diffusible components. These systems have fascinating properties: First, they can form truly self-organized patterns in the absence of initial asymmetries, thereby generating *de novo* positional information (Meinhardt and Gierer, 2000). Second, a large variety of pattern forms (e.g. spots and stripes, Fig. 1a) can be generated by simply varying the reaction and diffusion parameters (Kondo and Miura, 2010; Marcon and Sharpe, 2012), which could in principle account for the structural and morphogenetic diversity of life forms. Third, RD patterns are responsive to external perturbations and possess the remarkable ability to regenerate after perturbations (Gierer and Meinhardt, 1972; Kondo, 2017; Müller and Nüsslein-Volhard, 2016).

The dynamics of a number of biological systems that are compatible with the principles underlying the RD mechanism have recently been quantitatively studied (Diego et al., 2018; Marcon et al., 2016; Nakamasu et al., 2009; Raspopovic et al., 2014; Scholes et al., 2019; Zheng et al., 2016), but it remains unclear how commonly the principles of RD systems are actually realized in living systems. Qualitative similarities between *in silico* RD patterns and *in vivo* patterns are generally not sufficient to conclude the involvement of an RD mechanism (Hiscock and Megason, 2015). In addition, owing to its simplicity, Turing's theory has been questioned by developmental biologists: How could a simple two-component RD system explain the complex morphogenetic program orchestrated by multiple genetic and molecular regulators? Due to mathematical and computational limitations it has been difficult to address this long-standing criticism and to extend simple RD models to realistic multi-component biological processes. Here, we discuss how these challenges have been tackled in recent studies, yielding new insights into the mechanisms and conditions that lead to pattern formation in realistic RD systems.

2. The local self-activation and lateral inhibition proposal

The simplest and most well-known example of an RD system is the *activator-inhibitor system*. The activator-inhibitor system, coined by Hans Meinhardt and Alfred Gierer (Gierer and Meinhardt, 1972), consists of two diffusible components that interact through specific reactions.

* Corresponding author. Systems Biology of Development Group, Friedrich Miescher Laboratory of the Max Planck Society, 72076, Tübingen, Germany.
E-mail address: patrick.mueller@tuebingen.mpg.de (P. Müller).

https://doi.org/10.1016/j.ydbio.2019.10.031
Received 26 June 2019; Received in revised form 29 October 2019; Accepted 29 October 2019
Available online 30 January 2020

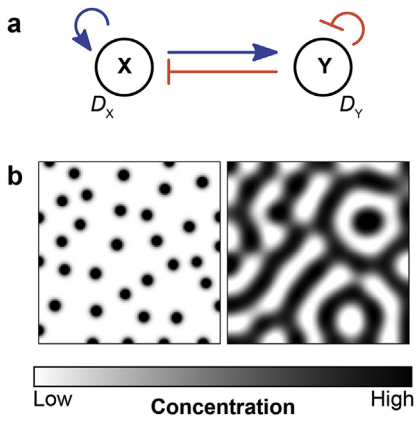

Fig. 1. The basic concept of reaction-diffusion (RD)-mediated pattern formation. (a) Network representation of a self-organizing activator-inhibitor system. The activator X promotes production of itself and of the inhibitor Y, while the inhibitor restricts activator production (arrow: activation, bar-headed line: inhibition). **(b)** Examples of two-dimensional Turing patterns generated using the activator-inhibitor network shown in (a) with the equations $\frac{\partial X}{\partial t} = D_X\nabla^2 X + \left(\frac{X^2}{1+K_X X^2} + X_0\right) \Big/ Y - \mu_X X$ and $\frac{\partial Y}{\partial t} = D_Y\nabla^2 Y + X^2 - \mu_Y Y$ (based on Meinhardt, 2012), where $D_X = 0.2$ and $D_Y = 10$ are the diffusivities of X and Y, $X_0 = 0.1$ is the basal production rate of X, and $\mu_X = \mu_Y = 5$ are the decay rate constants. The saturation constants are $K_X = 0$ for the spot pattern on the left and $K_X = 0.25$ for the stripe pattern on the right.

Turing had already laid the foundation for such a two-component system with linear reaction terms (Turing, 1952), but Meinhardt and Gierer proposed a model with biochemically more realistic nonlinear reaction terms (Gierer and Meinhardt, 1972; Meinhardt, 2012; Turing, 1952). As shown in Fig. 1a, in this model the activator X with diffusivity D_X promotes its own synthesis and that of the inhibitor Y with diffusivity D_Y, which in turn inhibits the activator and itself. Interestingly, this system can self-organize from an initially uniform distribution to give rise to stationary periodic patterns of activator and inhibitor concentrations (Murray, 2013; Turing, 1952). Such patterns with a characteristic periodicity or wave-length are termed *Turing patterns* (Fig. 1b, Box 1).

For the network in Fig. 1a, the well-established condition for Turing pattern formation is that the inhibitor must have a much larger diffusivity than the activator ($D_Y \gg D_X$) (Murray, 2013; Turing, 1952). This differential diffusivity requirement led to the proposal of the famous *local self-activation and lateral inhibition* model by Meinhardt and Gierer (Gierer and Meinhardt, 1972; Meinhardt and Gierer, 2000). According to this model, the local auto-activation by the activator and the lateral inhibition of its activity by the antagonist is crucial for self-organized pattern formation. The model postulates that the activator amplifies small random fluctuations to form a local concentration maximum, which subsequently leads to the activation of the inhibitor. Next, the inhibitor dampens the concentration increase in the vicinity of the activator peak. The higher diffusivity of the inhibitor also allows the incipient activator peaks to grow by 'siphoning out' inhibitor molecules from the peak region. Outside the range of lateral inhibition, another activator peak can then arise leading to the sequential emergence of a stationary periodic pattern. Intuitively, it appears that this simple principle could also be extended to more complex multi-component RD systems by considering two groups of interacting substances: the slow diffusers and the fast diffusers. The slow diffusers would have a shorter range and taken together should form an auto-activating module, whereas the latter with a larger range should form an inhibitory module (Meinhardt and Gierer, 2000). However, in reality this intuitive approach is not applicable to more complex systems (Marcon et al., 2016). In the following, we describe recent studies of multi-component RD systems that have provided evidence against the generality of the local self-activation and lateral inhibition proposal by showing that the differential diffusivity condition can be partially or even completely relaxed. These recent studies place the emphasis on feedback loops rather than individual activator and inhibitor molecules and provide a new way to understand RD systems.

3. Insights into RD systems beyond two-component Turing systems

Owing to advances in technology, recent computational analyses of multi-component RD systems have revealed novel insights into pattern formation mechanisms. The apparently simple local self-activation and lateral inhibition concept and the conditions underlying two-component systems get increasingly complex with the number of network components. A graph-theoretical approach can help to dissect these complex networks into functional modules (Diego et al., 2018; Marcon et al., 2016), and we introduce the relevant terminology in Box 2 to illustrate the key concepts of this approach.

3.1. Relaxation of diffusivity constraints

To describe the rules to relax the differential diffusivity constraints, we consider three-component systems with two diffusible nodes and one non-diffusible node (Fig. 2), where a node represents an interacting molecular species within the network. In contrast to classical two-component models with exclusively diffusible molecules (Fig. 1a), such an extended network more realistically reflects biological systems, in which signal transduction components such as membrane-bound receptors and nuclearly localized transcription factors are cell-autonomous and therefore non-diffusible with respect to all other cells within the tissue. Consistent with the central tenets derived from the analysis of two-component systems, the network topology shown in Fig. 2a requires differential diffusivity for Turing pattern formation (Marcon et al., 2016). This means that the two molecules must diffuse at very different rates, a condition that is difficult to implement in biological systems (Müller et al., 2013; Rogers and Müller, 2019). The need for differential diffusivity stems from the trade-off between the stability and the instability conditions (Box 1), i.e. the system must be stable without diffusion but become destabilized in the presence of diffusion. Using linear stability analysis and graph theory (Box 1 and Box 2), it was shown that if all nodes complementary to the stabilizing linear subgraphs (l-subgraphs) of the same size as the destabilizing module are diffusible, then differential diffusivity is required to produce a diffusion-driven instability (Diego et al., 2018). For the network in Fig. 2a, the subgraph containing nodes 2 and 3 is *destabilizing* and has a size of 2. The only *stabilizing* subgraph with a size of 2 is the cycle containing nodes 1 and 2. The complementary node to this stabilizing subgraph is node 3, which is diffusible. Thus, this network requires differential diffusivity ($D_1 > D_3$) for Turing pattern formation. It naturally follows that systems with only diffusible nodes always require components with different diffusivities. Systems that require differential diffusivity for self-organized pattern formation are termed Type I networks (Marcon et al., 2016).

Recent studies of multi-component RD systems have shown the presence of additional network types. Already more than two decades ago, it had been speculated that the differential diffusivity requirement might be relaxed in multi-component RD systems (White and Gilligan, 1998), and it was subsequently demonstrated that the addition of a non-diffusible node in a three-node RD system can indeed allow self-organized pattern formation with equal diffusivities (Klika et al., 2012). More recently, a systematic analysis of realistic multi-component systems revealed numerous three- and four-node RD networks, in which differential diffusivity is no longer required for pattern formation (Marcon et al., 2016). For example, the network topology shown in Fig. 2b can generate Turing patterns even with *equal* diffusion coefficients of the diffusible nodes ($D_1 \geq D_3$). This network type is called a Type II system. Furthermore, Type III networks (e.g. Fig. 2c) can lead to pattern formation without any diffusivity constraints ($D_1 \geq D_3$ or $D_1 < D_3$) (Marcon et al., 2016).

Box 1

| Conceptual basis for pattern formation in self-organizing RD systems.

The RD mechanism amplifies local fluctuations in the concentration of initially nearly homogenously distributed molecules by a diffusion-driven instability. For the formation of Turing patterns, two key conditions must be satisfied: First, the *stability condition* requires that the system reaches a stable and spatially homogeneous steady state in the absence of diffusion. In other words, when the diffusivities of activator and inhibitor are set to zero, the activator and inhibitor should maintain uniform and constant concentrations. Second, the *instability condition* dictates that in the presence of diffusion, the steady state must become destabilized by a so-called diffusion-driven instability, leading to the amplification of small random concentration fluctuations to yield a unique and time-invariant Turing pattern (Murray, 2013; Turing, 1952).

The figure below (Box 1) depicts this mechanism in a one-dimensional spatial domain. Initially, the concentration of a diffusible component exhibits minor fluctuations around a homogeneous steady state over this one-dimensional domain. The fluctuations can be interpreted as being composed of waves of different wavelengths (q). For instance, the spatial wave in panel **(a)** below is composed of six distinct waves. Under the stability and instability conditions given by reaction and diffusion parameters, the system can undergo a diffusion-driven instability, which amplifies these fluctuations. Importantly, different fluctuations are amplified at different growth rates. Over time, the fluctuation with the highest growth rate dominates and gets fixed, such as the wave with wavelength q_5 shown in panel **(b)** below.

Based on a mathematical technique termed *linear stability analysis*, the stability and instability conditions for Turing pattern formation are expressed in terms of eigenvalues of the linearized equations, which provide the growth rates of intrinsic spatial fluctuations. Mathematically, the eigenvalues can be plotted as a function of each wave mode (fluctuation) to obtain the *dispersion relation*, whose shape determines the nature of the diffusion-driven instability (Cross and Hohenberg, 1993). According to the stability condition, all eigenvalues should be negative in the absence of diffusion, i.e. when all species are assumed to be non-diffusible; therefore, no fluctuation can grow without diffusion. Furthermore, the instability condition requires that in the presence of diffusion at least one eigenvalue is positive. Typically, the spatial mode with the maximum real part of the eigenvalue will be the one that grows fastest – leading to the growth of a fluctuation and a diffusion-driven instability.

In the classical activator-inhibitor RD network (Fig. 1), if the inhibitor has a sufficiently higher diffusivity than the activator, the system can cause a diffusion-driven instability leading to spatial pattern formation. Note that the same fluctuation is amplified simultaneously for both the activator and the inhibitor, and the resulting pattern has a single wavelength. In two-dimensional spatial domains, complex patterns with periodic stripes, spots, etc. can emerge (panel **(c)** below), and the periodicity is determined by the underlying wavelength of the pattern. In three dimensional geometries, RD systems can create tubules and laminar sheets (Bansagi et al., 2011).

Schematic depiction of the self-organizing RD mechanism. (a) Initial random perturbations in the concentration of a molecular species consist of numerous different waves, where q_i indicates the wavelength. **(b)** A Turing pattern is established by selective amplification of a specific wave form. Here, the wave with wavelength q_5 is amplified. **(c)** Periodic Turing patterns in one dimension (a wave) and in two dimensions (stripes and spots).

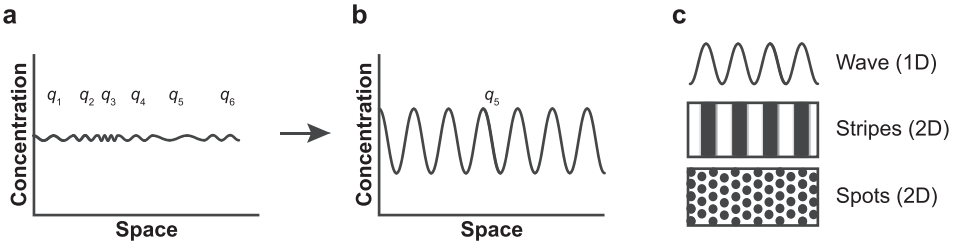

A comprehensive graph-theoretical analysis (Box 2) has provided an explanation for these surprising findings (Diego et al., 2018). The position of non-diffusible nodes in a network transforms the instability condition (Box 1) and thus determines whether a system requires differential diffusivity for pattern formation. Specifically, to implement a Type II system – which allows for equal diffusivities of the diffusible network components (Fig. 2b) – at least one stabilizing *l*-subgraph of the same size as the destabilizing module needs to have a complementary non-diffusible node (Box 2). In Fig. 2b, the stabilizing *l*-subgraph is the cycle between nodes 1 and 3, and its complementary node (node 2) is non-diffusible. To implement a Type III system – which has no restrictions on the diffusivities of the diffusible network components (Fig. 2c) – the destabilizing module needs to be the *l*-subgraph of the smallest size that has only diffusible complementary nodes (Diego et al., 2018). In Fig. 2c, the cycle between nodes 2 and 3 is the destabilizing *l*-subgraph of the smallest size (size 2) with a diffusible complementary node (node 1). Here, the Type III system (Fig. 2c) can be distinguished from the Type II system (Fig. 2b) by noting that the non-diffusible node (node 2) in the Type III system lacks the auto-regulatory feedback that is present in the Type II system. In short, placing non-diffusible nodes complementary to stabilizing modules and forming part of the destabilizing modules yields network topologies with relaxed diffusivity constraints. Thus, the Type I, Type II and Type III networks, which may superficially appear to be very similar (Fig. 2a–c), can require diverse biophysical properties based on variations in network topology.

It has been postulated that the interactions between diffusible and non-diffusible nodes lower the *effective* diffusion coefficient of the diffusible activator, thus indirectly relaxing the diffusivity constraint (Zheng et al., 2016). However, this proposed mechanism fails to explain pattern formation at equal diffusivities. It rather seems that non-diffusible nodes act as *capacitors* that integrate the input from diffusible nodes (Marcon et al., 2016). In classical two-component networks, differential diffusivity drives the system away from a homogeneous and stable equilibrium to generate patterns. In multi-component Type II and Type III networks, this is achieved by the non-diffusible nodes that can quickly amplify small perturbations since they are not subject to the equilibrating effect of diffusion (Marcon et al., 2016). The existence of these newly discovered network topologies strongly argues against the previous local self-activation and lateral inhibition hypothesis, which stated that differential diffusivity is a *conditio sine qua non* for

Box 2

| Graph-theoretical framework for the analysis of multi-component RD systems.

Mincheva and Roussel pioneered a graph-theoretical approach to analyze Turing instabilities in multi-component RD systems (Mincheva and Roussel, 2006), which inspired a new framework to identify self-organizing systems and to group the network components into functional modules (Diego et al., 2018; Marcon et al., 2016). Here, we only introduce the most basic concepts needed for our discussion, and further details can be found in Marcon et al. (2016) and Diego et al. (2018).

The figure below (Box 2) shows a four-node interaction graph. The nodes represent diffusible or non-diffusible molecules, and their interactions are depicted by the edges connecting these nodes (arrow: activation, bar-headed line: inhibition). An activating edge has a positive weight, whereas an inhibitory edge has a negative weight (denoted by the constants k_{ij}, which give the activation (+) or inhibition (−) rates of the node j by the node i). For the graph-theoretical analysis, the interaction graph is simplified by defining linear subgraphs (*l*-subgraph). An *l*-subgraph is a set of one or more disjoint cycles of the interaction graph, where a cycle is a closed path spanning one or more nodes. The nodes that are excluded from a subgraph are *complementary* nodes with respect to the subgraph. The size of an *l*-subgraph is the total number of nodes it comprises. In the figure, *l*-subgraphs 1, 2, and 3 are composed of one cycle each and have sizes 1, 2, and 3, respectively. The *l*-subgraph 4 is composed of two cycles and has a size of 4. The weight of a cycle is the product of the weights of all of its edges. The weight of an *l*-subgraph is the product of the weights of its cycles multiplied by -1 if the number of cycles in the subgraph is an odd number. The *l*-subgraphs with positive weights are stabilizing, and those with negative weights are destabilizing. In brief, subgraphs with overall inhibitory effect are stabilizing, whereas subgraphs with overall activating effect are destabilizing.

Interestingly, the stabilizing and destabilizing subgraphs directly determine the stability and instability conditions (Box 1). The pattern formation conditions are satisfied when i) the stabilizing interactions dominate in the absence of diffusion, and ii) destabilizing interactions dominate when certain nodes are diffusible. Importantly, it is not the whole graph structure that matters, but only linear subgraphs – which drastically simplifies the analysis of complex networks. Thus, the graph-theoretical framework provides a basis for deriving the pattern formation conditions of RD systems.

Graph-theoretical framework for RD networks. An interaction graph is a graph-theoretical representation of the network topology and consists of nodes and the interactions among them. A four-node interaction graph and its linear subgraphs are shown. Notations are the same as in Fig. 2.

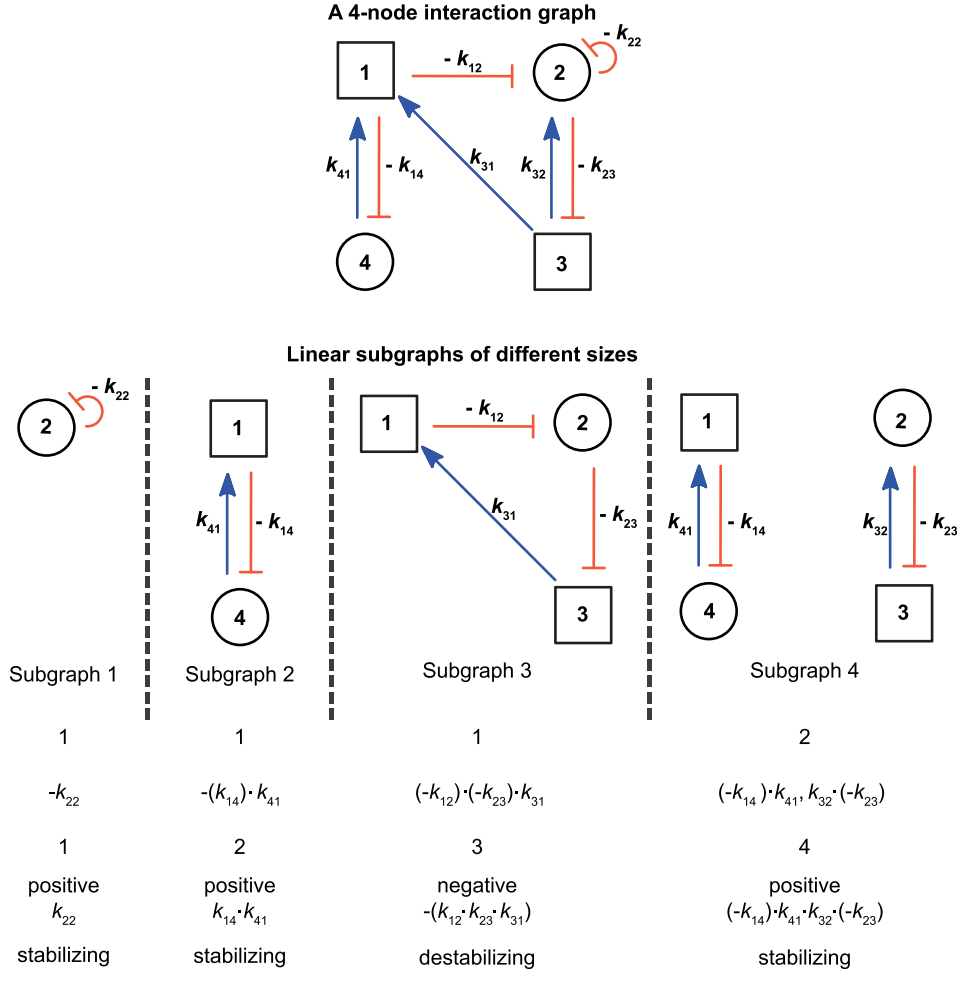

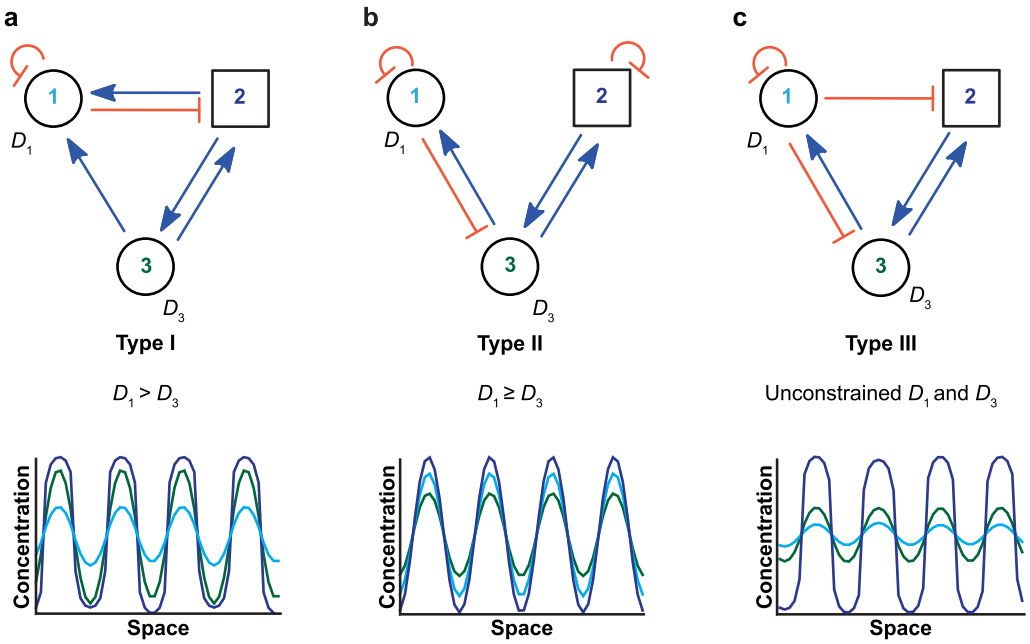

Fig. 2. Relaxation of diffusivity constraints. (a–c) Examples of Turing network types based on diffusivity constraints along with representative 1D patterns for each network generated using RDNets (Marcon et al., 2016). Circle: diffusible node, square: non-diffusible node, D_i: diffusion coefficient, arrow: activation, bar-headed line: inhibition.

self-organized biological pattern formation.

Surprisingly, Type II and Type III networks constitute the majority – about two thirds – of minimal three-node and four-node RD networks (Marcon et al., 2016). These discoveries therefore open new possibilities for RD networks to be considered as working hypotheses in experimental and computational modeling studies of biological patterning systems. Moreover, the multi-component network topologies also offer enticing models for synthetic biological patterning systems (see below).

3.2. Discovery and design of robust Turing networks

It has been thought that Turing networks require intricate fine-tuning of the reaction and diffusion parameters to yield stable patterns (Butler and Goldenfeld, 2011; Diego et al., 2018). This idea, known as the *robustness problem*, was mainly based on the analysis of a limited number of RD systems such as the activator-inhibitor system, which necessitated large differences in diffusivities of the involved components (Gierer and Meinhardt, 1972; Turing, 1952). However, as discussed above, recent insights obtained from the analysis of realistic multi-component RD systems enable the design and discovery of robust Turing networks with smaller differences or even equal diffusivities of the involved signaling molecules. Here, we discuss general principles that can aid in the discovery and the design of robust RD networks. For the sake of clarity and simplicity, we define robust systems as networks that give rise to self-organizing Turing patterns for a wide range of reaction-diffusion parameters. According to this definition, robust RD networks have a large Turing space (Fig. 3).

Recent studies have shown that robust network topologies tend to possess common elements (Diego et al., 2018; Marcon et al., 2016; Scholes et al., 2019; Zheng et al., 2016). Although these studies used different mathematical formulations, they suggest very similar rules for the design of robust Turing networks. While some studies used Hill-type reaction terms (Scholes et al., 2019; Zheng et al., 2016), others incorporated linear reaction terms with cubic saturation kinetics (Diego et al., 2018; Marcon et al., 2016). It has been suggested that in order to build robust multi-component Turing networks, one should 1) use as many classical two-component activator-inhibitor modules (Fig. 1a) as possible in the network, and 2) add additional regulations that complement the existing core topology (Zheng et al., 2016). Consistent with this view, it was demonstrated by numerical screening that the presence of core network topologies similar to the activator-inhibitor module could confer robustness to the RD system (Scholes et al., 2019). Moreover, networks with competitive Hill-type reaction kinetics are on average more robust, albeit less common, than networks with non-competitive Hill-type kinetics (Scholes et al., 2019). However, the generality of these insights may be limited by the numerical screening approach with specific choices of kinetic functions (Scholes et al., 2019; Zheng et al., 2016), where only partial parameter spaces of small networks can be explored

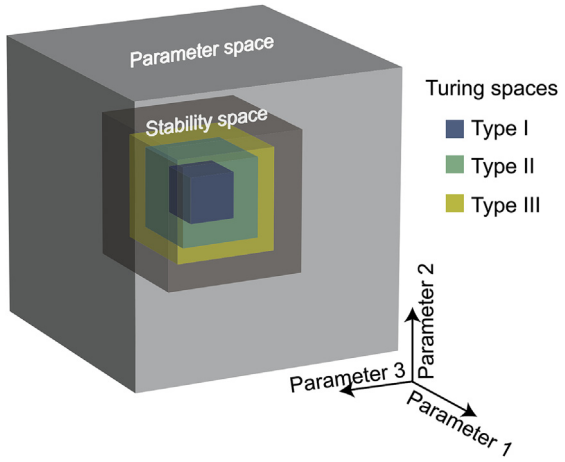

Fig. 3. Simplified schematic of the relationship between network robustness and network types. The parameter space comprises all possible parameter combinations. The stability space comprises only those parameter combinations that fulfill the stability condition. All networks within the same topological family have the same stability space, but their Turing space varies according to their network type. In this simplified schematic, the multi-dimensional parameter space only encompasses three parameters for ease of visualization, but the exact sizes and shapes of the spaces are more intricate for most systems.

due to computational constraints. In contrast, any network regardless of the choice of kinetic functions or number of links can be studied with a graph-theoretical approach (Diego et al., 2018; Marcon et al., 2016). This has shown that the network type based on diffusivity constraints (Type I, II or III) is a key determinant of the Turing space (Fig. 3) (Diego et al., 2018). Minimal Turing networks can be grouped into topological families, where a topological family refers to a group of networks with the same distribution of edges among the nodes (e.g. 7 topological families for three-node networks with 6 positive or negative interactions) (Diego et al., 2018; Marcon et al., 2016). All networks within a topological family have the same stability space, i.e. the steady state of all of these networks is stable for the same parameter space (Fig. 3). The Turing space occupies a portion of the stability space, and this portion increases from Type I to Type II networks and from Type II to Type III networks. Thus, topological family and network type govern the robustness of a given Turing network. Type II and Type III networks are more robust than Type I networks because the diffusivity constraint largely constricts the Turing space in Type I systems. This implies that Type II and III networks are more suitable for the design of robust synthetic RD systems. Furthermore, the large degree of robustness of Type II and Type III networks also suggests that that they are more likely to be adapted for pattern formation processes during evolution (Marcon et al., 2016). Importantly, even larger systems that have more than the minimal number of links can be analyzed within the framework of measuring the stability and instability volume. However, since this approach is based on linear reaction terms, the accuracy of the robustness prediction for a particular system will depend on how well the linear approximation holds far from equilibrium.

3.3. Rules to determine the phase relationships in spatial patterns

Another important aspect of RD networks is their ability to generate spatially overlapping (in-phase) or mutually exclusive (out-of-phase) patterns (Fig. 4a and b), similar to the observed patterns of biological regulators (Marcon et al., 2016). These spatial expression patterns can act as critical cues to relay positional information for the determination of cell fates during development as well as for the maintenance of differentiated cell populations (Green and Sharpe, 2015).

Interestingly, the pattern phases are governed solely by the nature of regulatory interactions among the components, and it is possible to predict the overlap between species from the network topology without the need for numerical simulations (Diego et al., 2018). Fig. 4a and b depict the classical activator-inhibitor and substrate-depletion RD models, respectively (Murray, 2013). In the activator-inhibitor model the activator induces itself and the inhibitor, whereas in the substrate-depletion model the activator (node 1 in Fig. 4b) consumes the substrate (node 2 in Fig. 4b) for its own activation, leading to the depletion of the substrate by fueling the activator. The in-phase pattern produced by the activator-inhibitor network (Fig. 4a) can be altered to an out-of-phase pattern (Fig. 4b) by simply changing the signs of all edges emerging from and coming to any chosen node. For example, in Fig. 4a inverting the edges emerging from node 1 (a to $-a$, and c to $-c$) followed by an inversion of the edges coming to the same node ($-b$ to b, and $-c$ to c), converts the initial activator-inhibitor network to the substrate-depletion network, thereby altering the pattern phasing. Note that the self-regulatory loops (auto-activation or auto-inhibition) remain unchanged as they undergo a double inversion (c to $-c$, and $-c$ to c). This principle can be extended to multi-component RD systems. For an N-node RD network, there are 2^{N-1} possible phase relationships, which can be comprehensively analyzed by systematically altering the network topologies (Diego et al., 2018). For three-node networks, for example, there are $2^{3-1} = 4$ possible phase relationships (Fig. 4c). Thus, the network topology is the key determinant of pattern phases. In the future, these insights could be used to design synthetic self-organizing tissues with any combination of spatially overlapping or separated gene expression patterns (see below).

4. Novel theoretical frameworks for RD systems

4.1. Moving local equilibria

The classical approach of analyzing Turing instabilities solely based on the shape of dispersion relations (Cross and Hohenberg, 1993), which describe the growth rates of different spatial perturbations around a homogeneous steady state (Box 1), has major limitations: The dispersion relation approach is applicable only in special cases where the growth of small spatial perturbations around a steady state is driven by nearly linear interactions (Halatek and Frey, 2018; Smith and Dalchau, 2018a). However, in real biological scenarios, patterning information can be generated before reaching a stable steady state (Bergmann et al., 2007), and it has been proposed that the stability of the homogeneous steady state is not a necessary condition for Turing pattern emergence (Smith and Dalchau, 2018a). To address these limitations associated with the analysis of linearized RD systems, Halatek and Frey proposed a mathematical framework, which can predict the behavior of nonlinear dynamical systems that are far from the steady state (Halatek and Frey, 2018). It is based on the idea that the dynamics of a mass-conserving system – a system where the molecules do not exit the system but are interconverted – can be studied by partitioning it into local spatial compartments and analyzing the stability of the local equilibrium or steady state of each compartment. In the absence of diffusion-driven mass redistribution, the compartments are not coupled leading to stable local equilibria. However, in the presence of diffusion the diffusive coupling of the compartments leads to lateral mass redistribution, thereby causing the displacement of local equilibria. These *moving local equilibria* have been postulated to guide the emergence of self-organized patterns and to scaffold their final shape (Halatek and Frey, 2018). This framework has been successfully applied to the MinD-MinE patterning system, which controls the positioning of the division plane in bacteria, and in the future it will be interesting to explore the generality of the key role of lateral mass redistribution in the emergence of spatial order for multi-component RD networks.

4.2. Wave-pinning for self-organizing scale-invariant patterns

Another prime example of a mass conserving system is the network that controls eukaryotic cell polarization in response to external stimuli (Mori et al., 2008). A simplified two-component model of this system considers two forms of a cell-polarity regulator: i) a highly diffusible cytosolic inactive form, and ii) a membrane-localized active form with 100-fold lower diffusivity. Mass conservation in this system arises from the interconversion of active and inactive forms, which are restricted within a cell. At a given concentration of the inactive form, the active form concentration has the bistable steady states S- and S_+ (Fig. 5). A transient polarizing signal of sufficient amplitude can bias the initially homogeneous distribution of the active form to drive the emergence and propagation of a wave due to the bistable reaction kinetics (Fig. 5). The propagation of the wave is halted, i.e. the wave is *pinned*, when the interconversion rates of the two forms are balanced and the final polar pattern is established (Fig. 5) (Mori et al., 2008). The wave-pinning framework for single cells has recently been extended to models for the patterning of whole tissues, e.g. for the Nodal/Lefty system that regulates early *Xenopus* embryogenesis (Middleton et al., 2013), and the theory might also be relevant for pattern formation in organoids (Ishihara and Tanaka, 2018).

It is currently unclear whether wave-pinning and classical diffusion-driven instabilities represent different mechanisms (Brena-Medina and Champneys, 2014; Halatek and Frey, 2018; Trong et al., 2014; Verschueren and Champneys, 2017). Given the common ingredients of reaction and diffusion, the mechanisms are certainly related, but most importantly they can be clearly distinguished based on their different patterning behaviors: While classical Turing patterns have a fixed wavelength leading to different numbers of peaks in differently sized

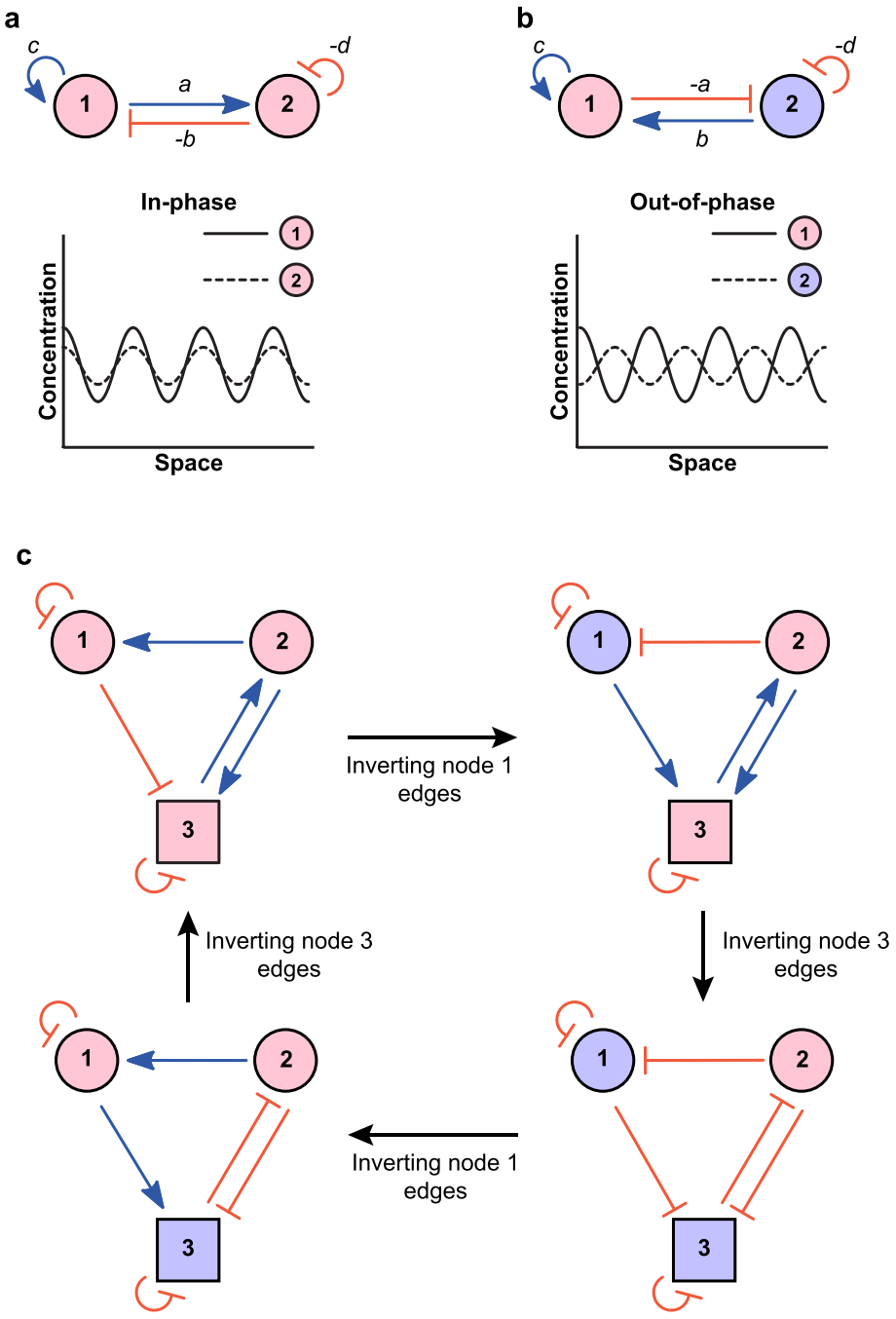

Fig. 4. Rules to determine pattern phases. (a) The activator-inhibitor network topology produces in-phase Turing patterns. **(b)** The substrate-depletion network topology produces out-of-phase Turing patterns. **(c)** An example showing the generation of all possible phase relationships for three-node networks. Nodes with the same color indicate that they are in-phase. Notations are the same as in Fig. 2.

domains, the dimensions of wave-pinning-induced patterns proportionately scale with the domain size (Diego, 2013; Ishihara and Tanaka, 2018; Mori et al., 2008) as experimentally observed in many biological patterning systems (reviewed in Čapek and Müller, 2019; Ishihara and Tanaka, 2018; Umulis and Othmer, 2013). Importantly, it has also been shown that is possible to systematically design an RD system that can only exhibit the behavior characteristic of wave-pinning – but not of Turing patterns – by analyzing the graph structure of the underlying network (Diego, 2013).

4.3. *Incorporating tissue mechanics and fluid flows*

A long-standing limitation of RD models is that they typically do not account for potential effects of tissue mechanics and extracellular fluid flows on pattern formation. A new model has recently addressed this limitation and provides a glimpse into a general framework of pattern formation based on the theory of biological mixtures (Ateshian, 2007). The new model incorporates the effects of two distinct phases within multicellular tissues: the poroelastic network of cells, and the extracellular fluid phase (Recho et al., 2018). In this biphasic model, the tissue architecture was assumed to be dependent on the concentration of signaling molecules: Activating signals would increase the local cell volume fraction relative to the extracellular phase, whereas inhibitory signals would decrease it (Recho et al., 2018). Thus, extracellular fluid movements could be guided by tissue mechanics depending on local changes in the cell volume fraction. The biphasic model predicted several

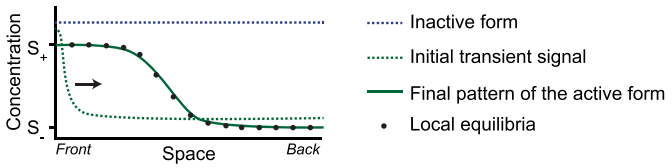

Fig. 5. Emergence of a wave-pinning pattern in a bistable reaction-diffusion system. A schematic wave-pinning pattern across the length of a cell or a tissue is shown. The active form distribution is polarized by a transient stimulus at the front of the domain. Consequently, the wave front of active form concentration propagates across the domain before it eventually arrests and 'pins'. The maxima and minima of the wave correspond to the top and bottom steady states (S_+ and S-), respectively, of the bistable system (Mori et al., 2008), and it was recently shown that wave propagation is driven by shifts in local equilibria (Halatek and Frey, 2018).

new types of instabilities that can lead to pattern formation, including self-organizing patterns driven by the active transport of signaling molecules along the extracellular fluid as well as the large-scale flow of cells themselves. Interestingly, patterning could even be achieved with a single signaling molecule, and the resulting patterns exhibited robust scaling properties to regulate tissue proportions in differently sized fields (Recho et al., 2018), similar to the properties of the wave-pinning model discussed above. The ability to achieve Turing instabilities with virtually any two-component reaction scheme (e.g. inhibitor-inhibitor interactions) is another fascinating property of this model, which could explain pattern formation in the absence of classical activator-inhibitor dynamics (Madzvamuse et al., 2015; Recho et al., 2018). Although many assumptions and predictions of this mathematical framework await experimental validation, the emerging ideas will likely inspire new advances in the field.

4.4. Model reduction approaches for RD systems

One of the major problems with the application of RD systems to model patterning is the complexity of biological networks. Biological networks usually possess a large number of interacting components. However, beyond four-node RD networks the computational power required for numerical analysis is enormous, and analytical solutions can be practically impossible for many research groups. In the following, we discuss how model reduction strategies have been employed to tackle these challenges.

Smith and Dalchau recently formulated a model reduction approach resembling a quasi-steady-state approximation (QSSA) (Smith and Dalchau, 2018a). QSSA assumes that in a system of chemical reactions the concentrations of chosen intermediate species remain constant. This can enable reduction of complex differential equations to much simpler algebraic equations. Using this approach, it is possible to eliminate all non-diffusible nodes from an N-node RD system with M diffusible nodes ($2 < M < N$). In simple terms, this is achieved by assuming that the non-diffusible species have equilibrium concentrations at all times, thus enabling their elimination from the system. Consequently, this approach preserves the characteristics of the parameter space to a large extent, i.e. the reduced system has the same stability space and Turing space as the original system. Furthermore, the pattern wavelength is unaffected by model reduction (Smith and Dalchau, 2018a). However, there are caveats to this approach. First, a reduced system that contains only diffusible nodes cannot form Turing patterns with equal diffusivities even if the original system can do so. Second, the system dynamics are not preserved upon model reduction, and the reduced model exhibits faster patterning dynamics due to the underlying mathematical assumptions. Third, this approach cannot be applied to RD systems in which all species are diffusible. Even with these limitations, the model reduction approach can be very useful when the main objective is to find pattern-forming parameters. Generally, very few species are cell non-autonomous and diffusible even in large biological networks, and this model reduction approach can allow the extraction of the Turing space with considerably less computational power in a short amount of time.

Another important concept that simplifies the application of Turing-like systems to biological patterning is the kernel-based Turing (KT) model (Kondo, 2017), which depends on the shape of an activation-inhibition kernel rather than on partial differential equations such as those shown in the legend for Fig. 1a. The KT model assumes that the local concentration of a patterning molecule in a tissue depends on net activating and inhibitory signals received from nearby cells. This approach reduces model complexity since it does not assume any molecular mechanism of activation or inhibition. In this model, the kernel function is a sum of two Gaussian functions, which defines the extent of activating and inhibitory signals received from a cell at a distance (Fig. 6a). The total signal received from the surrounding cells is obtained by mathematical integration of the kernel, which determines the synthesis rate of a patterning molecule that is degraded at a constant rate. Interestingly, these basic assumptions can lead to the spatial patterning of this molecule (Fig. 6b and c), thereby giving rise to spatial information and influencing the cellular state. The nature of the signal, its means of propagation, and the cellular state governed by the signal are not explicitly defined in the kernel function and must be determined based on the biological system of interest. For example, in the case of the striped patterns on adult zebrafish, the projections of the pigment cells (yellow xanthophores and black melanophores) might constitute the signal carriers that determine the cellular state of pigmentation (Kondo, 2017; Nakamasu et al., 2009), but the KT model can also incorporate potential contributions of diffusion since it is agnostic to molecular details. The activation-inhibition kernel can be informed experimentally by analyzing the dynamics in wildtype and activation (Aramaki and Kondo, 2018) or inhibition (Nakamasu et al., 2009) conditions, and the KT model is particularly useful as a guiding framework when the detailed molecular mechanisms underlying pattern formation are unknown.

5. Significance for developmental and synthetic biology

As described above, the network topology is crucial to understand the pattern formation conditions of RD systems. While the complete set of interactions and thus the network topology of real biological patterning systems under investigation is rarely known, frameworks like the KT model may provide a useful starting point. Additional factors that can influence pattern formation include intrinsic noise, delays in signal transduction, transcription and translation as well as the geometry of the system (Gaffney and Monk, 2006; Umulis and Othmer, 2012). Furthermore, developmental patterning systems are often strongly influenced by pre-patterns resulting from a biased distribution of maternal factors (reviewed in Rogers and Müller, 2019); as opposed to purely self-organizing systems with homogeneous initial conditions, *self-regulating* systems with interacting diffusible and non-diffusible factors and initial pre-patterns therefore often better describe developmental patterning (Rogers and Müller, 2019). In spite of these challenges, experiment-guided computational modeling of RD systems can not only provide crucial insights into mechanisms of biological patterning but also aid in building synthetic patterning systems as outlined below (for an excellent review with more biological examples, see Schweisguth and Corson, 2019).

Vertebrate digit patterning depends on the signaling molecules BMP and Wnt as well as the cell-autonomous transcription factor Sox9 (Badugu et al., 2012; Raspopovic et al., 2014). In the mouse limb bud, the expression of *Sox9* and the distribution of the BMP signal transducer pSmad overlap, whereas both Wnt signaling and *BMP* expression are out-of-phase with respect to *Sox9* expression (Fig. 7a). Based on these observations and the known interactions between BMP, Wnt and Sox9, a three-node Turing network was proposed to underlie digit patterning, in which BMP and Wnt are diffusible nodes and Sox9 is a non-diffusible node (Raspopovic et al., 2014) (Fig. 7b). Computer simulations of this three-node model recapitulated the observed expression patterns, except

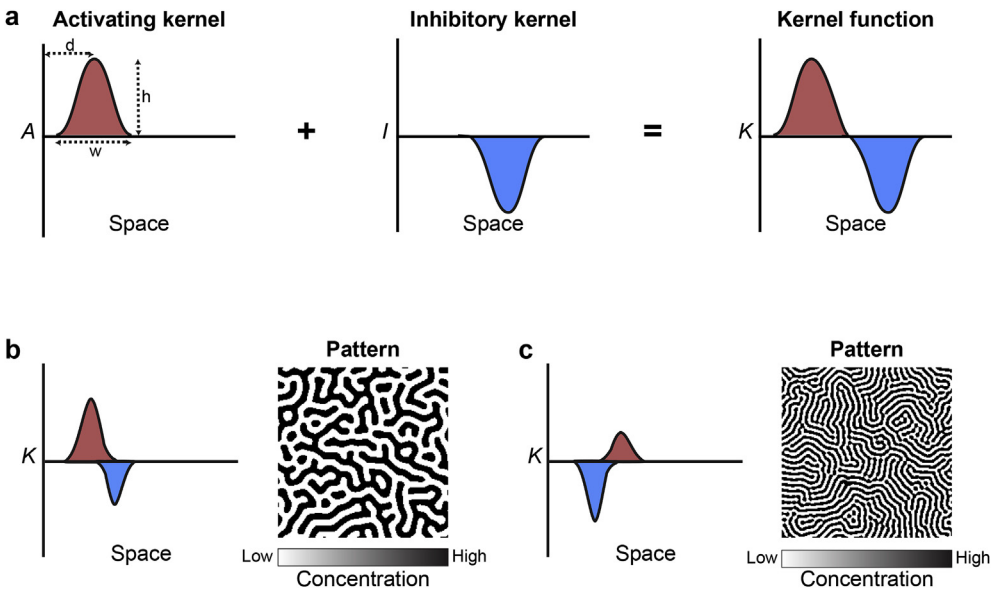

Fig. 6. Schematic depiction of pattern formation using kernel functions. (a) Summation of an activating spatial kernel *A* and an inhibitory spatial kernel *I* gives the spatial kernel function *K*. The amplitude (h), width (w), and distance (d) of the activating and inhibitory kernels are the defining characteristics of the kernel function. **(b,c)** Examples of kernel functions with their corresponding patterns simulated using the web-based KT model simulator (Kondo, 2017). Simulation parameters used in (b): activating kernel h = 15.5, w = 1.0, d = 4.13; inhibitory kernel h = -11.0, w = 0.81, d = 7.00. Simulation parameters used in (c): activating kernel h = 7.50, w = 1.0, d = 7.00; inhibitory kernel h = -15.0, w = 0.81, d = 4.13.

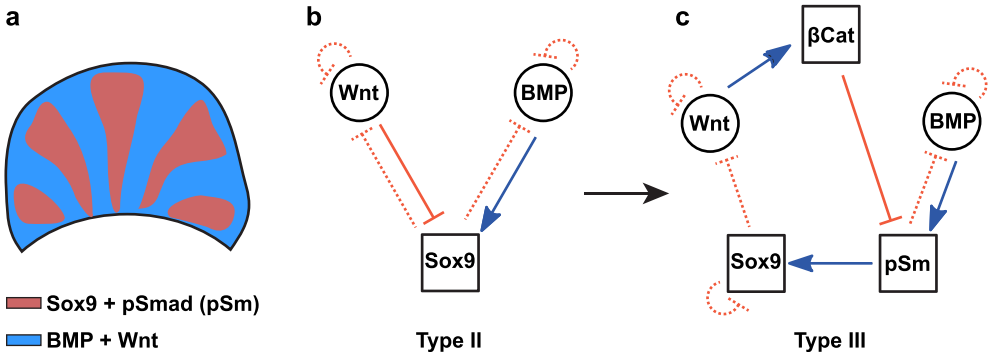

Fig. 7. Turing networks for vertebrate digit patterning. (a) A schematic representation of the in-phase and out-of-phase gene expression patterns in a developing vertebrate limb (pSmad and pSm indicate pSmad1/5/8). **(b)** Turing network employed in Raspopovic et al. (2014) to explain digit pattern formation. **(c)** Extension of the Turing network used in Marcon et al. (2016).

for the out-of-phase relationship between *BMP* expression and BMP signaling as measured by the distribution of the signal transducer pSmad. The three-node Turing network was subsequently extended to a five-node network (Fig. 5c) using the software RDNets (Marcon et al., 2016). The five-node network incorporated the BMP signal transducer pSmad and the Wnt signal transducer β-catenin as two additional non-diffusible nodes. In this updated model, indirect repression of Sox9 by β-catenin was able to explain all of the experimentally observed phase relationships, including the out-of-phase relation between *BMP* expression and BMP signaling. Additional negative feedbacks between Sox9, BMP and Wnt signaling were postulated (Marcon et al., 2016), but these interactions remain to be tested experimentally.

Attempts to construct synthetic RD systems capable of biological pattern formation have also been recently made in bacteria and mammalian cells (Davies, 2017; Karig et al., 2018; Luo et al., 2019; Santos-Moreno and Schaerli, 2018; Sekine et al., 2018). A synthetic activator-inhibitor genetic circuit was employed in bacteria to create stochastic patterns of fluorescent protein expression (Karig et al., 2018). These patterns were driven by a stochastic RD system and do not require classical Turing instabilities, thereby opening new opportunities for synthetic biological pattern formation. In another study, a synthetic mammalian pattern formation system was constructed (Sekine et al., 2018), based on the known differential diffusivity of the signaling molecules Nodal and Lefty (Müller et al., 2012; Rogers and Müller, 2019). However, this synthetic activator-inhibitor system could only generate irregular patterns of Nodal-positive cells surrounded by Nodal-negative cells (Sekine et al., 2018). Many mechanistic details of pattern formation in the bacterial and mammalian systems remain unknown, and Santos-Moreno and Schaerli therefore recently stated that *"[…] the engineering of a genuine Turing system remains yet to be achieved*" (Santos-Moreno and Schaerli, 2018). Previous studies were conceptually limited to two-component synthetic networks and differential diffusivity, but it will also be interesting to explore synthetic biological pattern formation using multi-component RD systems with relaxed diffusivity constraints (Diego et al., 2018; Marcon et al., 2016; Smith and Dalchau, 2018b).

6. Summary

In the past decade, the theory of RD-mediated pattern formation has witnessed exciting new developments and novel theoretical insights. The discovery of multi-component Turing networks that do not require differential diffusivity has challenged the classical view of local self-activation and lateral inhibition. A new understanding of the differential diffusivity criterion and patterning robustness from the analysis of multi-component RD systems has opened unprecedented opportunities for the discovery of biological patterning systems and the design of robust synthetic self-organizing systems (Marcon et al., 2016; Smith and Dalchau, 2018b; Zheng et al., 2016). It is therefore possible that these recent insights may enable novel therapeutic advances for future tissue engineering approaches. However, many challenges in mathematically

modeling complex biological signaling networks remain: More realistic models will require the incorporation of important effects such as tissue mechanics and compartmentalization as well as the integration of large signal transduction cascades and their interactions. At the same time, our understanding of the mechanisms underlying pattern formation is dependent on simplified abstract models. Striking the proper balance between realistic physical models and mathematical abstraction will likely inspire new studies of self-organization to derive meaningful biological insights in the future.

Definitions

Parameter space - The multi-dimensional space comprising all possible parameter combinations (Fig. 3).

Stability space - The fraction of the parameter space that satisfies the stability condition, i.e. the system is stable at the homogeneous steady state under these parameters in the absence of diffusion (Box 1, Fig. 3).

Turing space - The fraction of the stability space that results in time-invariant Turing patterns (Fig. 3).

Robustness - The probability of randomly picking pattern-forming parameter combinations from the parameter space. The pattern-forming parameter combinations essentially constitute the Turing space. Hence, a larger Turing space yields a more robust RD network.

Acknowledgments

We thank Hans Othmer, Daniel Čapek and Mohammad ElGamacy for valuable discussions. This work was supported by the Max Planck Society and the ERC Starting Grant *QUANTPATTERN* (637840).

References

Aramaki, T., Kondo, S., 2018. Method for disarranging the pigment pattern of zebrafish by optogenetics. Dev. Biol. pii: S0012-1606(18) 30467–6.
Ateshian, G.A., 2007. On the theory of reactive mixtures for modeling biological growth. Biomechanics Model. Mechanobiol. 6, 423–445.
Badugu, A., Kraemer, C., Germann, P., Menshykau, D., Iber, D., 2012. Digit patterning during limb development as a result of the BMP-receptor interaction. Sci. Rep. 2, 991.
Bansagi Jr., T., Vanag, V.K., Epstein, I.R., 2011. Tomography of reaction-diffusion microemulsions reveals three-dimensional Turing patterns. Science 331, 1309–1312.
Bergmann, S., Sandler, O., Sberro, H., Shnider, S., Schejter, E., Shilo, B.-Z., Barkai, N., 2007. Pre-steady-state decoding of the Bicoid morphogen gradient. PLoS Biol. 5 e46–e46.
Brena-Medina, V., Champneys, A., 2014. Subcritical Turing bifurcation and the morphogenesis of localized patterns. Phys. Rev. E - Stat. Nonlinear Soft Matter Phys. 90, 032923.
Butler, T., Goldenfeld, N., 2011. Fluctuation-driven Turing patterns. Physical Review E 84, 11112.
Čapek, D., Müller, P., 2019. Positional information and tissue scaling during development and regeneration. Development. In press.
Cross, M.C., Hohenberg, P.C., 1993. Pattern formation outside of equilibrium. Rev. Mod. Phys. 65, 851–1112.
Davies, J., 2017. Using synthetic biology to explore principles of development. Development 144, 1146–1158.
Diego, X., 2013. On the theory of cell migration: durotaxis and chemotaxis, Departament de Resistència de Materials i Estructures a l'Enginyeria. Universitat Politècnica de Catalunya.
Diego, X., Marcon, L., Müller, P., Sharpe, J., 2018. Key features of Turing systems are determined purely by network topology. Phys. Rev. X 8, 021071.
Gaffney, E.A., Monk, N.A., 2006. Gene expression time delays and Turing pattern formation systems. Bull. Math. Biol. 68, 99–130.
Gierer, A., Meinhardt, H., 1972. A theory of biological pattern formation. Kybernetik 12, 30–39.
Green, J.B.A., Sharpe, J., 2015. Positional information and reaction-diffusion: two big ideas in developmental biology combine. Development 142, 1203–1211.
Halatek, J., Frey, E., 2018. Rethinking pattern formation in reaction-diffusion systems. Nat. Phys. 14, 507–514.
Hiscock, T.W., Megason, S.G., 2015. Mathematically guided approaches to distinguish models of periodic patterning. Development 142, 409–419.
Ishihara, K., Tanaka, E.M., 2018. Spontaneous symmetry breaking and pattern formation of organoids. Curr. Opin. Struct. Biol. 11, 123–128.
Karig, D., Martini, K.M., Lu, T., DeLateur, N.A., Goldenfeld, N., Weiss, R., 2018. Stochastic Turing patterns in a synthetic bacterial population. Proc. Natl. Acad. Sci. 115, 6572.
Klika, V., Baker, R.E., Headon, D., Gaffney, E.A., 2012. The influence of receptor-mediated interactions on reaction-diffusion mechanisms of cellular self-organisation. Bull. Math. Biol. 74, 935–957.
Kondo, S., 2017. An updated kernel-based Turing model for studying the mechanisms of biological pattern formation. J. Theor. Biol. 414, 120–127.
Kondo, S., Miura, T., 2010. Reaction-diffusion model as a framework for understanding biological pattern formation. Science 329, 1616–1620.
Luo, N., Wang, S., You, L., 2019. Synthetic pattern formation. Biochemistry 58, 1478–1483.
Madzvamuse, A., Ndakwo, H.S., Barreira, R., 2015. Cross-diffusion-driven instability for reaction-diffusion systems: analysis and simulations. J. Math. Biol. 70, 709–743.
Marcon, L., Diego, X., Sharpe, J., Müller, P., 2016. High-throughput mathematical analysis identifies Turing networks for patterning with equally diffusing signals. eLife 5, e14022.
Marcon, L., Sharpe, J., 2012. Turing patterns in development: what about the horse part? Curr. Opin. Genet. Dev. 22, 578–584.
Meinhardt, H., 2012. Turing's theory of morphogenesis of 1952 and the subsequent discovery of the crucial role of local self enhancement and long-range inhibition. Interface Focus 2, 407–416.
Meinhardt, H., Gierer, A., 2000. Pattern formation by local self-activation and lateral inhibition. Bioessays 22, 753–760.
Middleton, A.M., King, J.R., Loose, M., 2013. Wave pinning and spatial patterning in a mathematical model of Antivin/Lefty-Nodal signalling. J. Math. Biol. 67, 1393–1424.
Mincheva, M., Roussel, M.R., 2006. A graph-theoretic method for detecting potential Turing bifurcations. J. Chem. Phys. 125, 204102–204102.
Mori, Y., Jilkine, A., Edelstein-Keshet, L., 2008. Wave-pinning and cell polarity from a bistable reaction-diffusion system. Biophys. J. 94, 3684–3697.
Müller, P., Nüsslein-Volhard, C., 2016. Obituary: Hans Meinhardt (1938-2016). Development 143, 1231–1233.
Müller, P., Rogers, K.W., Jordan, B.M., Lee, J.S., Robson, D., Ramanathan, S., Schier, A.F., 2012. Differential diffusivity of Nodal and Lefty underlies a reaction-diffusion patterning system. Science 336, 721–724.
Müller, P., Rogers, K.W., Yu, S.R., Brand, M., Schier, A.F., 2013. Morphogen transport. Development 140 (8), 1621–1638.
Murray, J.D., 2013. Mathematical biology II: Spatial models and biomedical applications. Springer, New York.
Nakamasu, A., Takahashi, G., Kanbe, A., Kondo, S., 2009. Interactions between zebrafish pigment cells responsible for the generation of Turing patterns. Proc. Natl. Acad. Sci. 106, 8429–8434.
Raspopovic, J., Marcon, L., Russo, L., Sharpe, J., 2014. Digit patterning is controlled by a Bmp-Sox9-Wnt Turing network modulated by morphogen gradients. Science 345, 566–570.
Recho, P., Hallou, A., Hannezo, E., 2018. Theory of mechano-chemical patterning in biphasic biological tissues. Proc. Natl. Acad. Sci. 116, 5344–5349.
Rogers, K.W., Müller, P., 2019. Nodal and BMP dispersal during early zebrafish development. Dev. Biol. 447, 14–23.
Roth, S., 2011. Mathematics and biology: a Kantian view on the history of pattern formation theory. Dev. Gene. Evol. 221, 255–279.
Santos-Moreno, J., Schaerli, Y., 2018. Using synthetic biology to engineer spatial patterns. Advanced Biosystems 3, 1800280.
Scholes, N.S., Schnoerr, D., Isalan, M., Stumpf, M.P.H., 2019. A comprehensive network atlas reveals that Turing patterns are common but not robust. Cell Systems 9, 243–257 e244.
Schweisguth, F., Corson, F., 2019. Self-organization in pattern formation. Dev. Cell 49, 659–677.
Sekine, R., Shibata, T., Ebisuya, M., 2018. Synthetic mammalian pattern formation driven by differential diffusivity of Nodal and Lefty. Nat. Commun. 9, 5456.
Smith, S., Dalchau, N., 2018a. Beyond activator-inhibitor networks: the generalised Turing mechanism arXiv 1803.07886.
Smith, S., Dalchau, N., 2018b. Model reduction enables Turing instability analysis of large reaction–diffusion models. J. R. Soc. Interface 15, 20170805.
Trong, P.K., Nicola, E.M., Goehring, N.W., Kumar, K.V., Grill, S.W., 2014. Parameter-space topology of models for cell polarity. New J. Phys. 16, 065009–065019.
Turing, A.M., 1952. The chemical basis of morphogenesis. Philosophical Transactions of the Royal Society (part B) 237, 37–72.
Umulis, D.M., Othmer, H.G., 2012. The importance of geometry in mathematical models of developing systems. Curr. Opin. Genet. Dev. 22, 547–552.
Umulis, D.M., Othmer, H.G., 2013. Mechanisms of scaling in pattern formation. Development 140, 4830–4843.
Verschueren, N., Champneys, A., 2017. A model for cell polarization without mass conservation. SIAM J. Appl. Dyn. Syst. 16, 1797–1830.
White, K.A.J., Gilligan, C.A., 1998. Spatial heterogeneity in three-species, plant-parasite-hyperparasite, systems. Philos. Trans. R. Soc. Biol. Sci. 353, 543–557.
Zheng, M.M., Shao, B., Ouyang, Q., 2016. Identifying network topologies that can generate Turing pattern. J. Theor. Biol. 408, 88–96.